

NRL Report 7371

**Stress-Corrosion Cracking
of High-Strength Steels
and Titanium Alloys**

R.W. Judy and R.J. Goode

Strength of Metals Branch
Metallurgy Division

March 13, 1972

Approved for public release; distribution
unlimited

DOCUMENT CONTROL DATA - R & D

(Security classification of title, body of abstract and indexing annotation must be entered when the overall report is classified)

1. ORIGINATING ACTIVITY (Corporate author) Naval Research Laboratory Washington, D.C. 20390		2a. REPORT SECURITY CLASSIFICATION UNCLASSIFIED	
		2b. GROUP	
3. REPORT TITLE STRESS-CORROSION CRACKING OF HIGH-STRENGTH STEELS AND TITANIUM ALLOYS			
4. DESCRIPTIVE NOTES (Type of report and inclusive dates) A special summary report on continuing problems.			
5. AUTHOR(S) (First name, middle initial, last name) Ralph W. Judy, Jr., and Robert J. Goode			
6. REPORT DATE March 13, 1972	7a. TOTAL NO. OF PAGES 32	7b. NO. OF REFS 36	
8a. CONTRACT OR GRANT NO. NRL Problem M01-25	9a. ORIGINATOR'S REPORT NUMBER(S) NRL Report 7371		
8b. PROJECT NO. RR 022-01-46-5432	9b. OTHER REPORT NO(S) (Any other numbers that may be assigned this report)		
8c.			
8d.			
10. DISTRIBUTION STATEMENT Approved for public release; distribution unlimited.			
11. SUPPLEMENTARY NOTES		12. SPONSORING MILITARY ACTIVITY Department of the Navy (Office of Naval Research) Washington, D.C. 20360	
13. ABSTRACT One of the major problems of metal structures in the seawater environment is the growth of flaws by the stress-corrosion-cracking (SCC) mechanism. Environmental effects on the integrity of the structure are related both to SCC processes and to the inherent tolerance of the material for flaws at regions of high stresses. The Ratio Analysis Diagram (RAD) provides translations of fracture resistance properties of metals to expected structural performance; the RAD has been modified to include analyses of the effects of SCC. The significance of section-size effects on the results of SCC tests based on linear-elastic analysis methods and expected structural behavior are included on the modified diagram, which is called the Dual-SCC RAD. Examples of several current high-strength steels and titanium alloys are referenced to the Dual-SCC RAD to illustrate its use.			

14. KEY WORDS	LINK A		LINK B		LINK C	
	ROLE	WT	ROLE	WT	ROLE	WT
Stress-corrosion cracking Ratio Analysis Diagram Titanium alloys High strength steels						

CONTENTS

Abstract	ii
Problem Status	ii
Authorization	ii
NOMENCLATURE	1
INTRODUCTION	1
SCC DEFINITION AND MEASUREMENT	2
RATIO ANALYSIS DIAGRAMS	8
ANALYSIS OF STEELS	14
ANALYSIS OF TITANIUM ALLOYS	18
SUMMARY	24
REFERENCES	24

ABSTRACT

One of the major problems of metal structures in the seawater environment is the growth of flaws by the stress-corrosion-cracking (SCC) mechanism. Environmental effects on the integrity of the structure are related both to SCC processes and to the inherent tolerance of the material for flaws at regions of high stresses. The Ratio Analysis Diagram (RAD) provides translations of fracture resistance properties of metals to expected structural performance; the RAD has been modified to include analyses of the effects of SCC. The significance of section-size effects on the results of SCC tests based on linear-elastic analysis methods and expected structural behavior are included on the modified diagram, which is called the Dual-SCC RAD. Examples of several current high-strength steels and titanium alloys are referenced to the Dual-SCC RAD to illustrate its use.

PROBLEM STATUS

This is a special summary and interpretative report covering the results of salt-water SCC studies. These studies are continuing.

AUTHORIZATION

NRL Problem M01-25
Project RR 022-01-46-5432

Manuscript submitted November 23, 1971.

STRESS-CORROSION CRACKING OF HIGH-STRENGTH STEELS AND TITANIUM ALLOYS

NOMENCLATURE

a	critical flaw size; depth of surface or edge crack
B	thickness
DT	Dynamic Tear (test)
LEFM	linear-elastic fracture mechanics
K	stress-intensity factor
K_{Ic}	critical plane-strain stress intensity
K_c	critical plane-stress stress intensity
K_Q	questionable or invalid K
K_{Isc}	threshold value of K above which SCC occurs
Wet K_Q	invalid value of K determined in a salt-water environment
σ	stress
σ_{ys}	yield strength
SCC	stress-corrosion cracking
R	resistance of a material to fast fracture
R-curve	fracture-extension-resistance curve
RAD	Ratio Analysis Diagram
Dual-SCC RAD	RAD modified for interpretations of SCC

INTRODUCTION

In addition to basic stress-analysis procedures, a structural designer must consider the effects of loading and environment that can cause preexisting flaws to grow to critical sizes. One of the primary problem areas for structures in the seawater environment is the rapid growth of flaws by the stress-corrosion-cracking (SCC) mechanism. There are several mechanical and chemical processes by which cracks grow under the combined effects of active environments and applied stresses; however, the macroscopic effect is crack propagation, which can be designated SCC for engineering purposes.

The degree of susceptibility of structural metals to SCC is not predictable from conventional mechanical property data; the only way to determine a material's relative sensitivity to environmental effects is to conduct specialized laboratory tests. In recent years, sharp-crack fracture-mechanics procedures have been extensively used to test structural metals for SCC sensitivity. These methods are employed for two reasons: (a) many materials (particularly titanium alloys) which are highly resistant to general corrosion can

be very sensitive to SCC if a sharp crack is present, and (b) the fracture mechanics type of test provides both a model of the most critical features (flaw plus stress level) of the structure and a relationship with established design practices against brittle fracture.

A large amount of SCC data based on fracture mechanics tests of steels and titanium alloys has been reported. Much of the data has not been analyzed in terms of applicability to failure-prevention procedures in design. At NRL combined analysis procedures for both fast-fracture and salt-water SCC have been developed; this report presents these procedures and interpretations for high-strength steels and titanium alloys.

SCC DEFINITION AND MEASUREMENT

Structural failures due to corrosion/stress-corrosion factors generally occur in the three distinct phases depicted in Fig. 1.

1. Pitting corrosion is the formation of small pits by chemical processes. Once formed, pits grow by a combination of fatigue and pitting corrosion to a size where SCC processes become effective.
2. Stress-corrosion cracking is the more rapid propagation of the crack due to the combined influence of the environment and the stress field.
3. Final failure by either unstable brittle fracture or ductile, overload fracture results from the growth of the crack to a size that is critical for the imposed stress level.

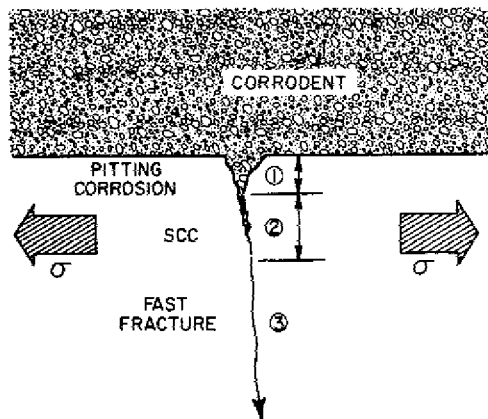


Fig. 1 — Illustrating the three phases of structural failure by corrosion and stress corrosion. All three phases are not necessary for failure in all cases.

Designers are concerned primarily with phases 2 and 3 of the process, i.e., the important factors are SCC and the final failure mode. Phase 1 can be excluded from a practical standpoint because the existence of cracks which are far larger than most corrosion pits is a certainty for many structures. Design against failure by SCC therefore requires either precluding rapid SCC propagation by material selection or predicting the rate of crack propagation and conditions for final fracture to assure a safe operating period.

A threshold effect in SCC behavior has been shown to exist for high-strength steels and titanium alloys. The threshold is dependent on the linear-elastic stress-intensity factor

K and is independent of applied stress for both steels (1) and titanium alloys (2). The stress-intensity factor is related to the product of stress σ and the square root of crack size a , i.e., $K = f(\sigma\sqrt{a})$. Applied K can be considered a mechanical condition analogous to applied stress; critical values of K describe characteristics of the material that can be expressed in terms of K . The characteristic K value at the threshold is called K_{Isc} and defines the level of applied K above which SCC will occur if the material is sensitive to environmental effects.

The physical events associated with measurement of SCC properties using fracture mechanics methods are illustrated in Fig. 2 using titanium alloys as an example. The fracture surface of a precracked specimen tested in an aqueous environment is shown in the center for a material that is sensitive to SCC. Starting with a constant load such that the applied K level is just above the characteristic K_{Isc} level, the SCC crack propagates until it becomes sufficiently large that the remaining ligament fractures. The photographs are electron microscope fractographs which illustrate the appearance of the various regions on a microscopic scale. Characteristically, fatigue fracture associated with precracking has

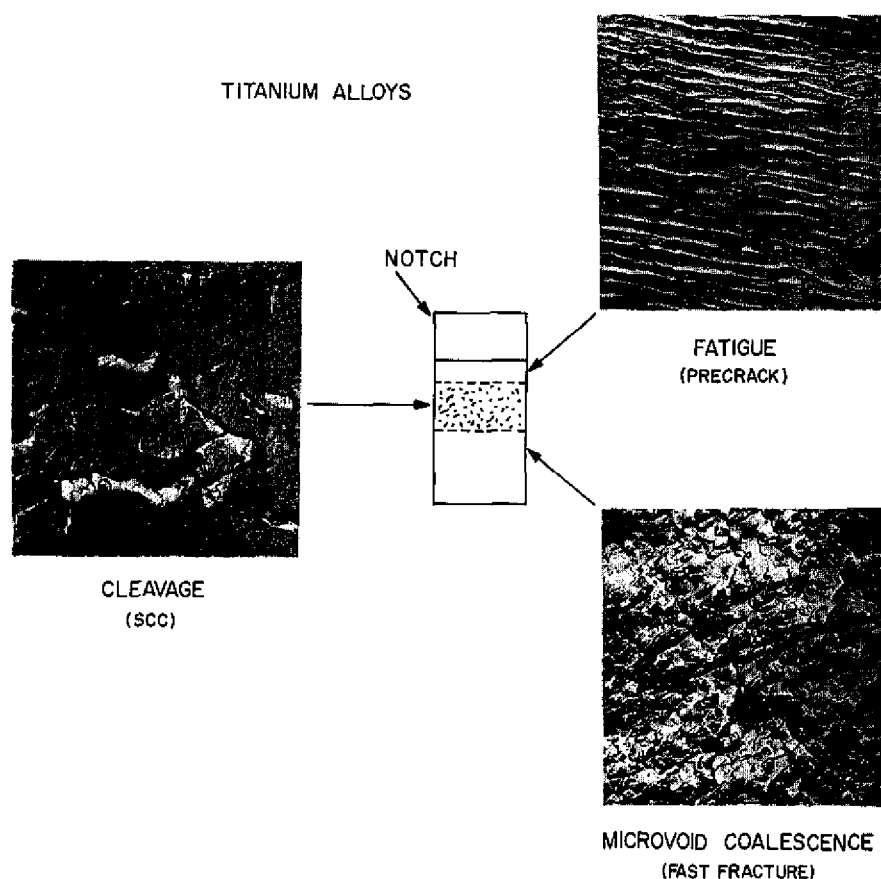


Fig. 2 — The processes of SCC in structural materials. The microscopic appearance of each type of fracture is illustrated for titanium alloys only. In materials that are not affected by SCC, the cleavage region is not present.

the striated appearance shown and fast fracture has the dimpled appearance denoted *microvoid coalescence*. In titanium alloys, SCC cracks propagate by a mechanism which results in cleavage fracture; the presence of cleavage on the fracture surface is evidence of occurrence of SCC. Identification of fracture processes in steels by electron microfractography is not as simple as for titanium alloys because cleavage and quasi-cleavage fracture modes are also associated with fast-fracture propagation in steels.

The above example applies to materials that are affected by the environment. If the materials are unaffected by the environment, the K level at which the specimen fractures is related to the fast-fracture properties of the metal rather than to the SCC properties.

To measure $K_{I_{SCC}}$ values for structural metals, any fracture mechanics specimen configuration can be used. The usual procedures involve loading a series of specimens at various applied K values with the hostile environment present and using bracketing methods between "break" and "no-break" specimens to determine $K_{I_{SCC}}$. The data are plotted as a function of time to show that the threshold has been measured, in that low values of K are not attained with longer test times. Test times of 1 to 3 hours are generally sufficient to attain threshold conditions in titanium alloys, while test durations of thousands of hours are not uncommon for steels.

Because of the relative simplicity of specimen preparation and test procedures, the cantilever bend test developed by Brown (3) is a widely used method where large numbers of specimens must be tested. The specimen configuration and the equation for calculating K along with test data for two titanium alloys are shown in Fig. 3. The examples are typical titanium alloys representing a sensitive (bottom) and an insensitive (top) condition. The reference point on the ordinate for each curve (denoted *dry*) is the K value determined in air. "No-break" points are indicated by arrows. In principle the difference between $K_{I_{SCC}}$ and the Dry K value indicates the severity of the environmental effect. A large difference indicates a large effect, whereas little or no difference indicates immunity to the environment.

Test specimen configurations other than the cantilever design are also used for SCC testing; however, for a given material, the same $K_{I_{SCC}}$ value is measured by each method. Three- and four-point bend specimens and center-cracked tensile panels are sometimes used for titanium alloys because of the relatively short test-time requirements. An interesting specimen configuration used for long-term tests of steels is the bolt-loaded WOL (wedge-opening-loaded) specimen developed by Novak (4). In this specimen, increasing crack length due to SCC results in SCC crack arrest at $K_{I_{SCC}}$ due to the rapidly decreasing values of applied K . Applied K decreases with crack growth because of the constant displacement and decreasing moment afforded by the bolt-loading system; thus several measurements of $K_{I_{SCC}}$ can be made on a single specimen by reloading arrested SCC cracks.

The advantage of using stress-intensity parameters to define SCC properties is that the $K_{I_{SCC}}$ value can be translated into critical flaw size vs stress level relations for crack growth by using the same equations and criteria defined by linear-elastic fracture mechanics (LEFM) that apply to the fast-fracture case. To properly use LEFM principles to characterize SCC properties of structural metals, plane-strain conditions must dominate the stress state because (a) LEFM is concerned only with plane strain, and (b) SCC is usually associated with plane strain. Plane-strain conditions are required across the major part of the crack front to assure applicability of the fracture mechanics equations for accurately defining the environmental effects. The stress state is determined by the degree of constraint

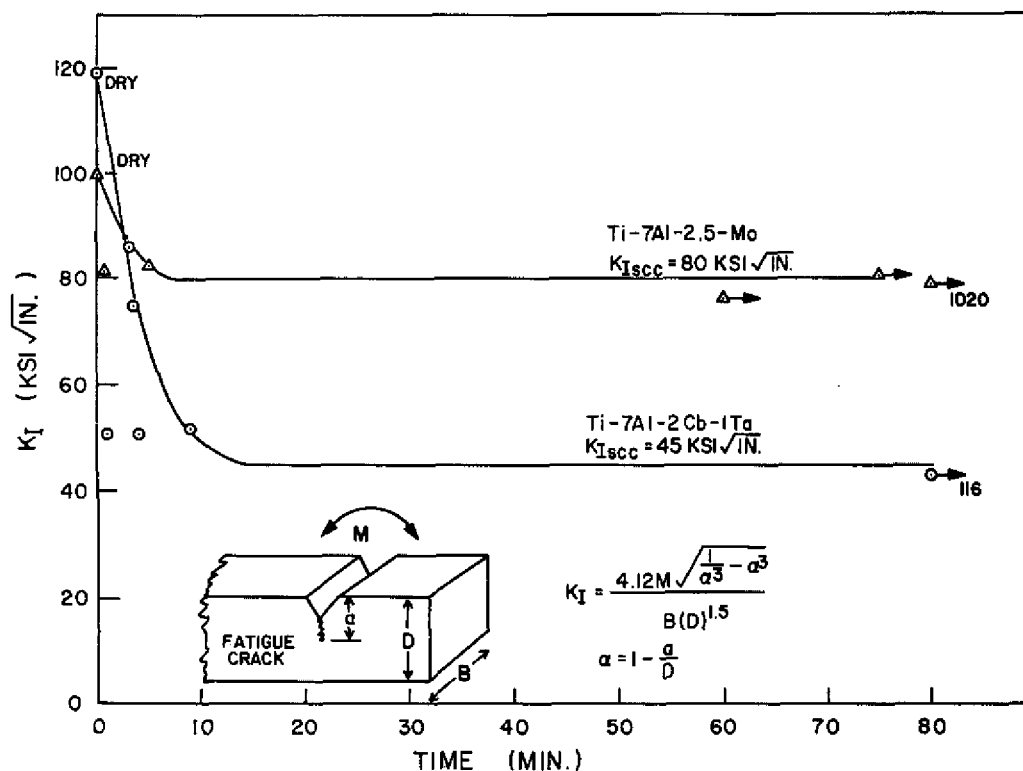


Fig. 3 — Typical SCC curves for titanium alloys sensitive to salt water (bottom) and insensitive to salt water (top). The cantilever bend type specimen and equation are also illustrated in this figure.

to plastic flow at the crack tip, which is a function of thickness (Fig. 4) and crack depth. The material at the center has a triaxial stress state which limits, or constrains, the flow of metal along the edge of the crack, while the surface material is free to flow (plane stress). A plane-strain condition exists when triaxial stress conditions predominate.

The fast-fracture resistance of a material can be measured in terms of the K parameter as either K_{Ic} or K_c , depending on the degree of constraint present in the specimen. A valid K_{Ic} value is independent of specimen geometry effects and therefore is a property of the material; plane-strain conditions are necessary for determining K_{Ic} . According to ASTM-recommended practice (5), the thickness requirement for a valid K_{Ic} measurement is

$$B \geq 2.5 (K_{Ic}/\sigma_{ys})^2 \quad (1)$$

where B = thickness and σ_{ys} = yield strength of material. Full-plane stress K_c values depend highly on specimen geometry and therefore are not a constant material property. This dependence occurs because the derivation of equations defining the K parameter assumes that the stress field can be represented as two dimensional and that plasticity effects at the crack tip are negligible; both of these conditions are violated by the plane stress state. K values that do not meet the suggested plane-strain criteria for validity are denoted K_Q , where the subscript Q denotes *questionable*. For the same reasons, only the SCC characterization data obtained under conditions of plane strain should be denoted as K_{Isc} values. Values of K obtained in a salt-water environment under plane-stress or plane-stress, mixed-mode conditions may not represent the characteristic value for the materials involved. Such

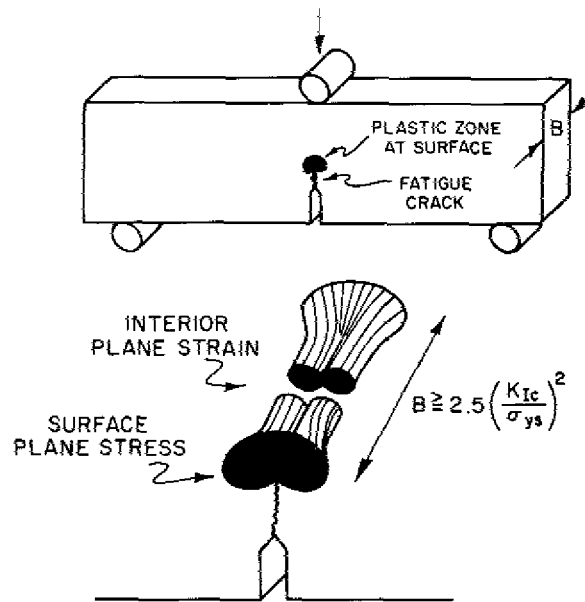


Fig. 4 — The effect of biaxial (specimen surface) and triaxial (specimen center) stresses on constraint of plastic zone formation at the tip of a crack

values of K are designated “wet K_Q .” The thickness requirements of the ASTM-recommended practice cited above presently provide the best guidance for valid K_{Isc} determinations. In the determination of minimum B , the value of K_{Isc} is used in place of K_{Ic} in Eq. 1.

Engineering applications of fracture mechanics are based on use of the equations describing stress level and flaw size combinations for different loading situations to predict the conditions necessary for the initiation of either brittle fracture or SCC propagation. The unique relation of LEFM is that $K = \alpha \sigma \sqrt{a}$ where σ = stress, a = flaw size, and α = constant related to geometry. An equation which describes a common part-through surface flaw case is

$$K = 1.1 \sigma \sqrt{\pi a/Q}, \quad (2)$$

where Q is the flaw geometry factor. If this is rewritten as

$$(K_{Isc}/\sigma_{ys})^2 \text{ or } (K_{Ic}/\sigma_{ys})^2 = 1.21 (\sigma/\sigma_{ys})^2 \pi a/Q, \quad (3)$$

where σ_{ys} = yield strength, it can be seen that the critical flaw size of a given shape is dependent only on the relative stress σ/σ_{ys} and the ratio of K_{Ic}/σ_{ys} or K_{Isc}/σ_{ys} . This relationship is depicted graphically in Fig. 5 for two selected flaw geometries and for a wide range of applied stress levels. It is cautioned that to use this chart, K_{Ic}/σ_{ys} or K_{Isc}/σ_{ys} applies only to materials which are sufficiently thick to maintain plane-strain conditions. (See Eq. 1.)

The SCC resistance of a material must be determined by comparison of the critical flaw size for fast fracture with the critical flaw size for SCC propagation which will eventually lead to fast fracture. This can be done for brittle materials by comparing K_{Isc} with

$$\left(\frac{K_{Ic}}{\sigma_{ys}}\right)^2 = 1.21 \frac{\pi a}{Q}$$

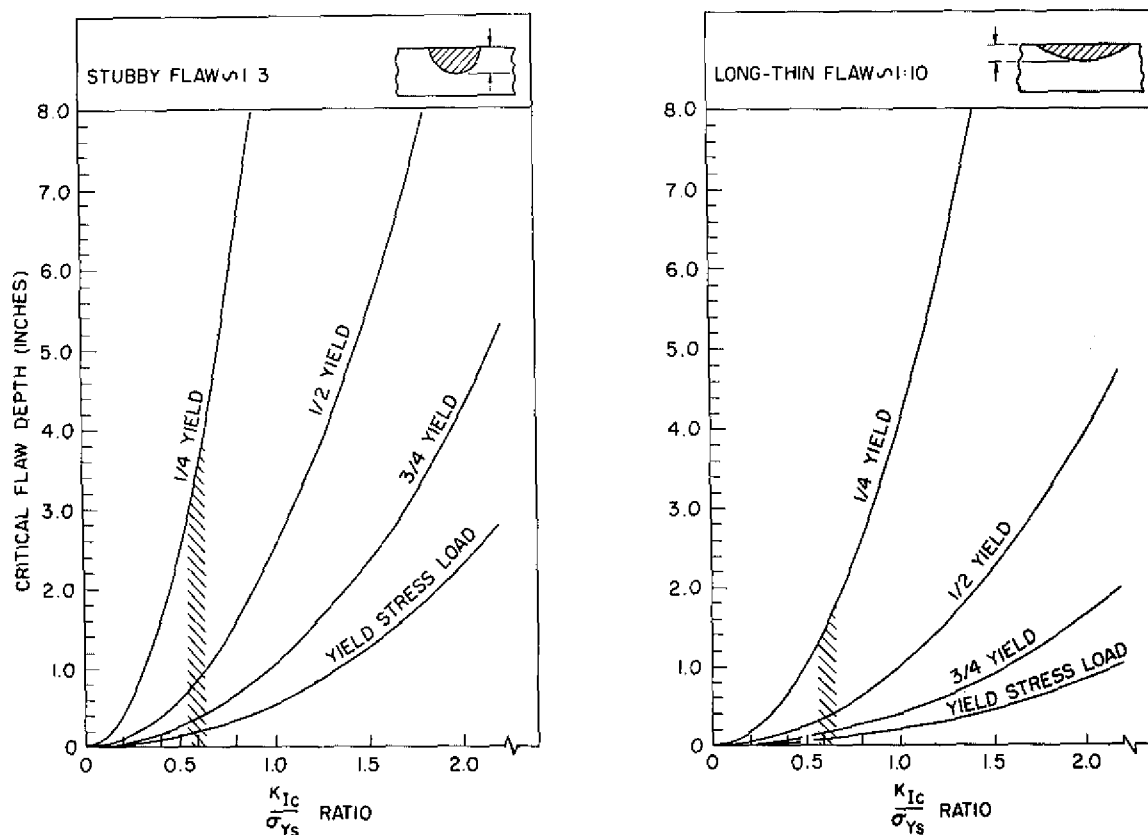


Fig. 5 — Relationships of flaw size and stress level for the initiation of unstable fracture in brittle metals as a function of the ratio K_{Ic}/σ_{ys}

K_{Ic} . For example, a value of K_{Isc} approaching the level of K_{Ic} signifies a high degree of SCC resistance; conversely, a low value of K_{Isc} compared to K_{Ic} indicates sensitivity to the environment. The K_{Isc} parameter by itself does not denote whether or not the material is sensitive to the environment. This is because K_{Isc} values cannot be larger than K_{Ic} ; i.e., materials with low K_{Ic} values will always be limited to low values of K_{Isc} . For ductile materials, comparison of the K_{Isc} value must be made with some other index of fast-fracture resistance such as DT or R-curve analyses (6-9). A third possibility is the case where a valid K_{Isc} cannot be measured. This condition denotes that specimen thickness is insufficient to maintain the plane-strain state; i.e., for that thickness the material would not be subject to SCC. If thicker sections of the material are of concern, then specimens of greater thickness must be used.

One of the factors observed in SCC testing of both steels and titanium alloys is that there is a decrease in the K value from Dry K_Q to Wet K_Q for almost all alloys, whether or not visible evidence of SCC propagation can be found. Furthermore, in some cases a K_{Isc} type of test on insensitive materials in normal laboratory air results in about the

same decrease. Thus, for some materials, test time tends to depress the measured K values to lower levels corresponding to plane strain such that very small flaws will be critical for fracture extension without positive assurance of the occurrence of SCC. Such effects are limited primarily to metals that are in the low to intermediate range of resistance to fast fracture; the level of Wet K_Q values for metals with high resistance to fracture and SCC are not depressed to the extent of attaining plane-strain conditions.

RATIO ANALYSIS DIAGRAMS

A simplified diagrammatic procedure for assessing the fast-fracture resistance of steels (10), titanium alloys (11), and aluminum alloys (12) has been established for several years. The basic diagram, called the Ratio Analysis Diagram (RAD), is based on a correlation between K_{Ic} and standard dynamic tear (DT) energy for 1-in.-thick plates and applies to all structural materials ranging from the most brittle to the most ductile. RADs for steels and titanium alloys are shown in Figs. 6 and 7, respectively.

The RAD framework is formed from the scales of yield strength vs DT energy and K_{Ic} . The most prominent features of the RAD are the limit lines and the system of lines of constant K_{Ic}/σ_{ys} ratio. The Technological Limit (TL) line represents the highest values of fracture resistance measured to date by either the DT or K_{Ic} tests over the entire yield-strength range; the lower bound represents the lowest levels of fracture resistance.

The system of ratio lines constructed from the scales of K_{Ic} and σ_{ys} provides a reference to the critical flaw size chart, Fig. 5; critical flaw sizes for a long, thin flaw for half-yield and full-yield loading are shown on the RAD for each ratio line. The ratio lines also divide the diagram into regions of expected ductile and brittle fracture for given material thicknesses in accordance with Eq. 1. Plane-strain limit ratio values, which denote the upper limit of LEFM applicability for given plate thicknesses, are shown in Table 1; some of these are also indicated on the RADs. The flaw detection limit shown to be at K_{Ic}/σ_{ys} ratio 0.3 corresponds to the minimum flaw size range that can confidently be expected to be located by existing nondestructive inspection methods. This limit then establishes the minimum point where LEFM can be reliably used.

To determine the influence of a particular environment on the structural performance of a material, it must first be recognized that SCC does not represent a degradation of the inherent resistance to fast fracture. However, if fracture toughness parameters and SCC parameters are both expressed in terms of a common index of structural performance, the effect of an environment can be accurately evaluated by the comparison of the two terms. Such an index is the critical flaw size as determined for fast fracture and for SCC at the same level of nominal stress. The RAD provides good engineering approximations of the flaw size vs stress requirements for the occurrence of fast fracture. Incorporation of the SCC characteristics of the same materials on this diagram permits a direct comparison of conditions for fast fracture and SCC. This dual SCC-fracture toughness RAD has been established for both high-strength steels and for titanium alloys (13,14).

The K_{Isc} data obtained from NRL studies and from the literature (15-36) for a wide variety of plate and weld metals in 3.5% salt water are shown in Fig. 8 for steels and in Fig. 9 for titanium alloys. The diagrams are the same as Figs. 6 and 7 with specific ratio lines that relate to thicknesses of test specimens indicated. Data points are coded according to nominal specimen thickness without consideration of side grooves. (Side grooves are

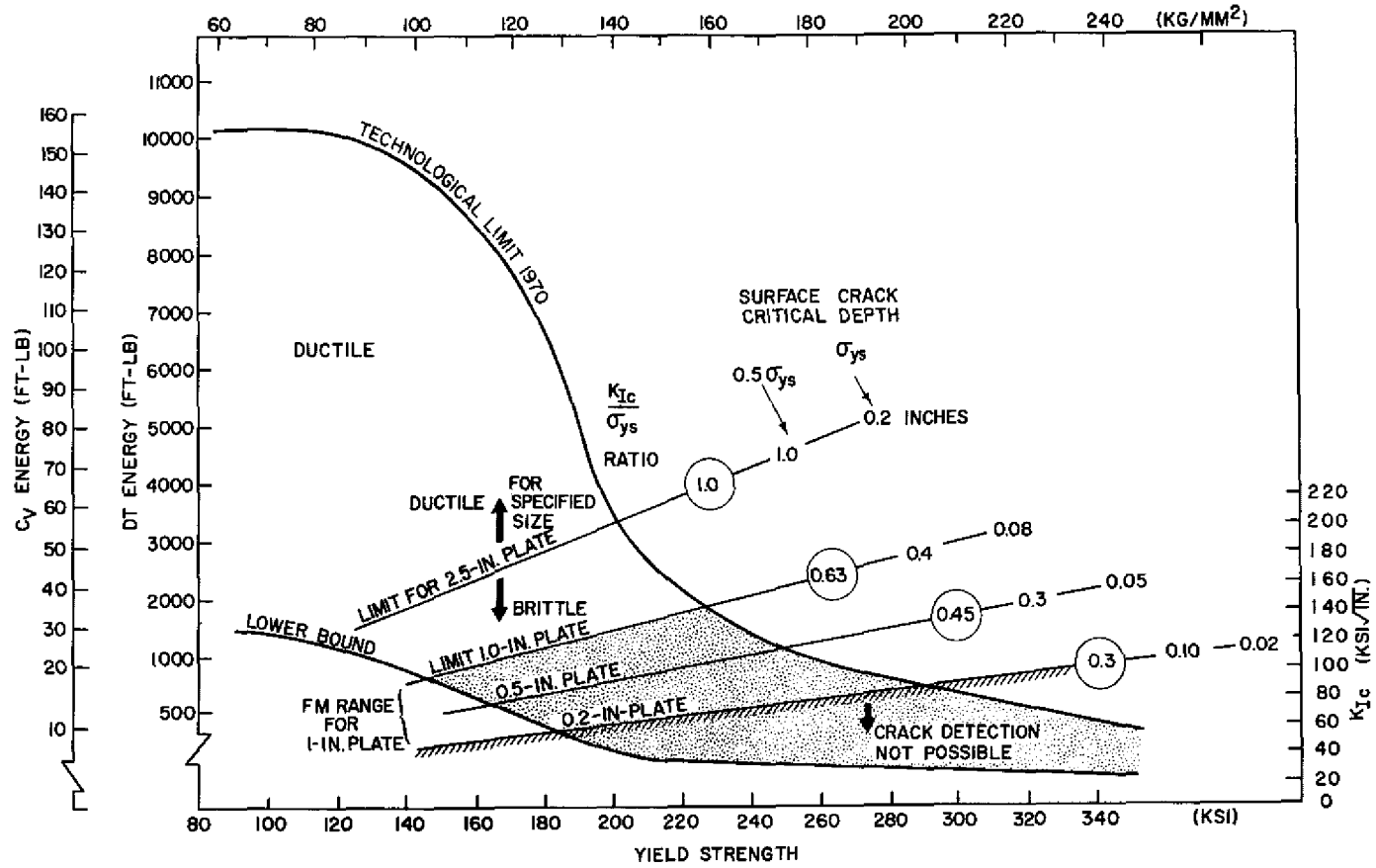


Fig. 6 — Ratio Analysis Diagram for high-strength steels; ratio limits for brittle fracture for specified section size

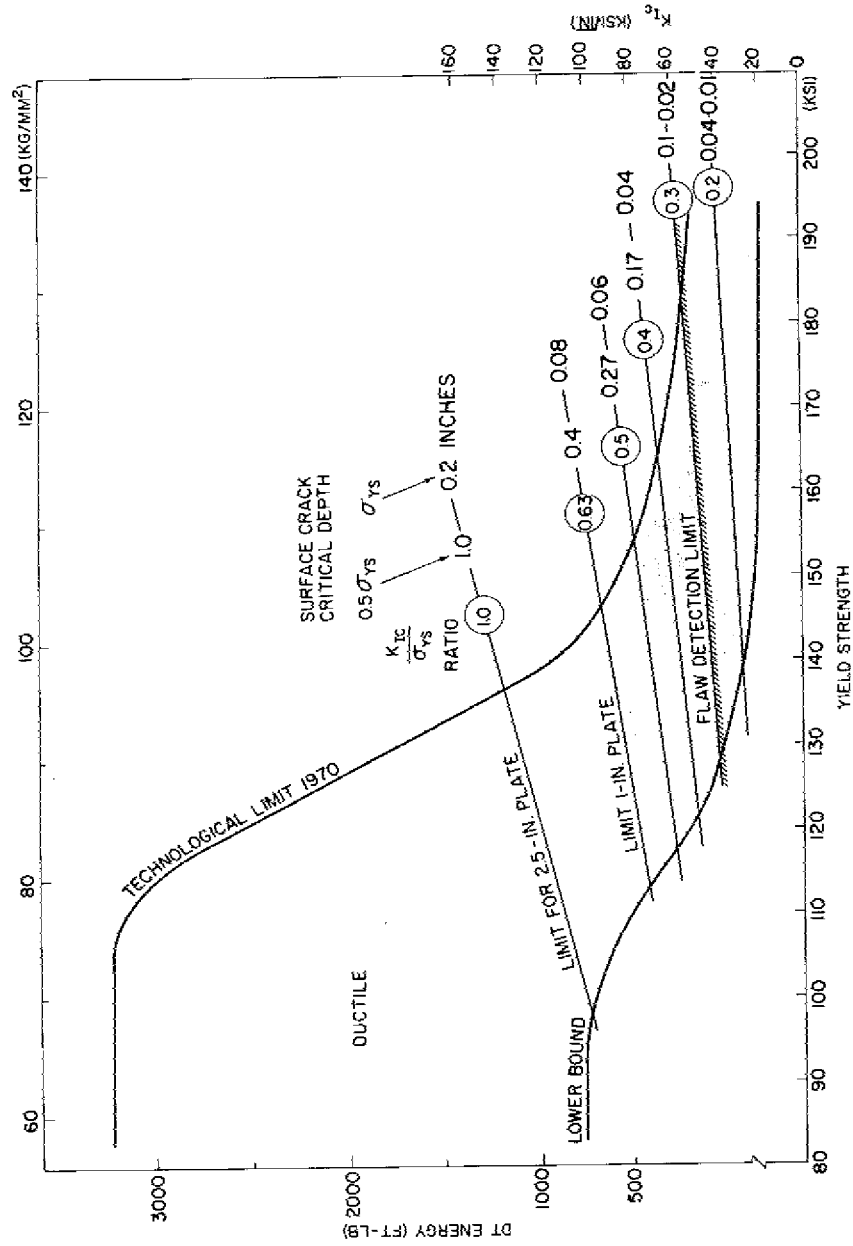


Fig. 7 — Ratio Analysis Diagram for high-strength titanium alloys

Table 1
Frangibility Limits

Plate Thickness B (in.)	Maximum Ratio K_{Ic}/σ_{ys} or K_{Isc}/σ_{ys} (in.) ^{1/2}
0.375	0.39
0.5	0.45
0.75	0.55
1.0	0.63
1.5	0.77
2.0	0.89
2.5	1.00
3.0	1.09
4.0	1.26
6.0	1.54
10.0	2.00

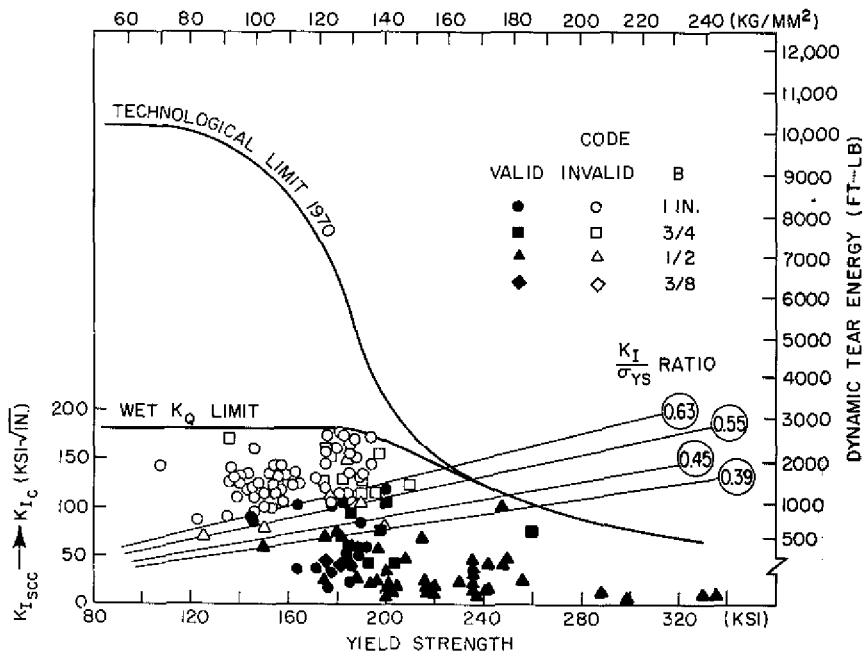


Fig. 8 — Dual-SCC RAD summary of K_{Isc} data for a spectrum of high-strength steels in a variety of thicknesses

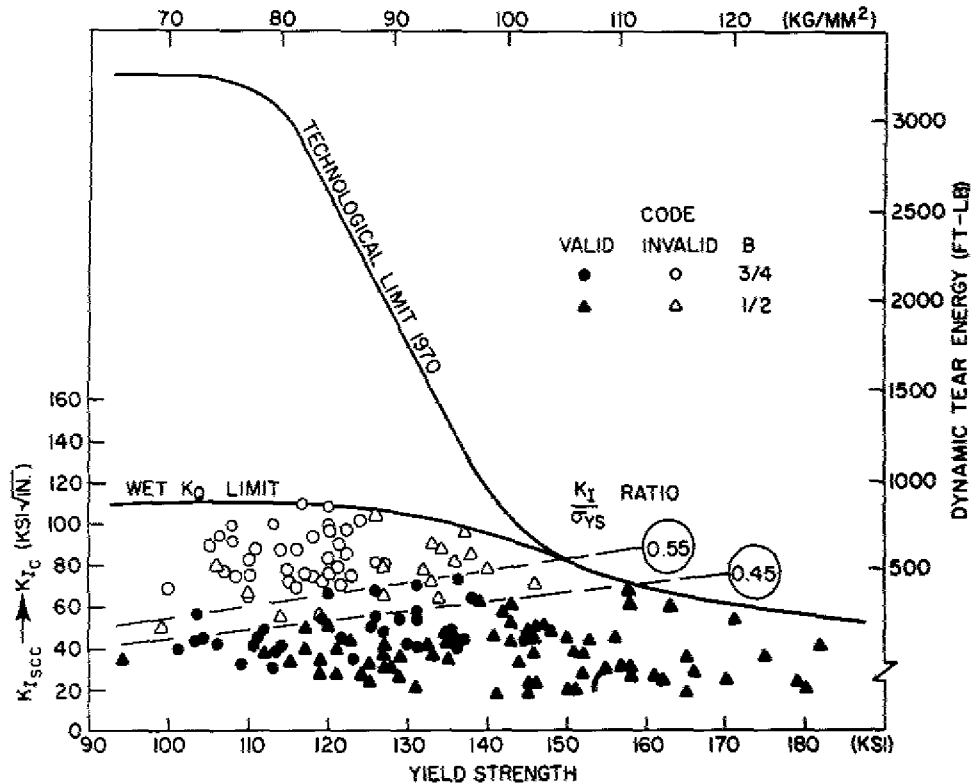


Fig. 9 — Dual-SCC RAD summary of $K_{I_{SCC}}$ data for titanium alloys at test specimen thicknesses of 0.5 and 0.75 in.

used to promote a straight crack front and to suppress shear-lip formation. Their use does not modify the thickness requirements for attainment of plane-strain conditions.) The maximum specimen thickness used was 1 in., corresponding to a limit ratio of 0.63 for plane strain.

The Wet K_Q limit is analogous to the Technological Limit for fast fracture in that it depicts the highest $K_{I_{SCC}}$ and Wet K_Q values reported. The same types of materials were used to establish the location of both limit lines. The effects of the lack of constraint due to insufficient specimen thickness can be shown by the relative positions of the Technological Limit and the Wet K_Q limit lines. At σ_{ys} levels of 220 and 240 ksi or greater the lines on the steel diagram converge. At this σ_{ys} level, even the best materials have a low level of fast-fracture toughness so that valid K_{Ic} numbers can be determined from 1-in.-thick plate; hence, the $K_{I_{SCC}}$ values for environmentally insensitive materials approach the K_{Ic} values. For titanium alloys this convergence occurs at a yield strength range of 140 to 150 ksi. In both cases the convergence of limit lines occurs at the bottom of the TL line strength transition.

Separation of the TL and Wet K_Q limit lines at yield strength values below the strength transition indicates the inability of the 1-in.-thick specimens to define fast-fracture and SCC resistance for the best materials in terms of fracture mechanics parameters. For example, the thickness requirements for steels are such that materials in the region defined by the highest part of the TL line do not manifest plane-strain fast fracture at thicknesses of 6 to

12 in. Thus, high K_{Isc} values reported for SCC specimens of 1-in. thickness or less should be viewed with suspicion when obtained for tough, high-strength materials.

The Dual-SCC framework of the RAD for high-strength steels in salt water is shown in Fig. 10 and for titanium in Fig. 11. The upper limit of strictly valid K_{Isc} measurements is indicated for thicknesses of 0.25, 0.5, and 1.0 in. as plane-strain limit lines for SCC as determined from Eq. 1. For the 1-in.-thick specimens, the plane-strain limit line for SCC corresponds to a K_{Isc}/σ_{ys} ratio of 0.63; for thinner specimens, the lines correspond to smaller ratios.

The plane-strain limit line for SCC for a given specimen thickness, in conjunction with the Wet K_Q limit line, defines a region where subcritical crack growth and fast-fracture conditions are either plane stress or plane stress/mixed mode. This is the Wet K_Q region, noted in Figs. 10 and 11 for 1-in.-thick sections, in which SCC may occur by advancing in the plane-strain ligament in the central portion of the specimen. Although such tunneling action would be indicative of SCC and Wet K_Q values could be obtained, the accuracy of such values cannot be determined. Critical flaw-depth stress-level requirements for SCC cannot be inferred for material falling in this region of the diagram. Specimens of increased thickness are required to accurately define the conditions for SCC for such materials. Increased specimen thickness would be expected to move the Wet K_Q region of the Dual-SCC RAD to higher K_I/σ_{ys} ratios; however, additional confirmation studies are required. In any event, the primary function of the Wet K_Q region of the diagram is to assure that a material's resistance to subcritical crack growth due to SCC in salt water is accurately represented by SCC test methods. Values which fall into the Wet K_Q region must be considered to give, at best, rough qualitative assessments of environmental sensitivity. Use of

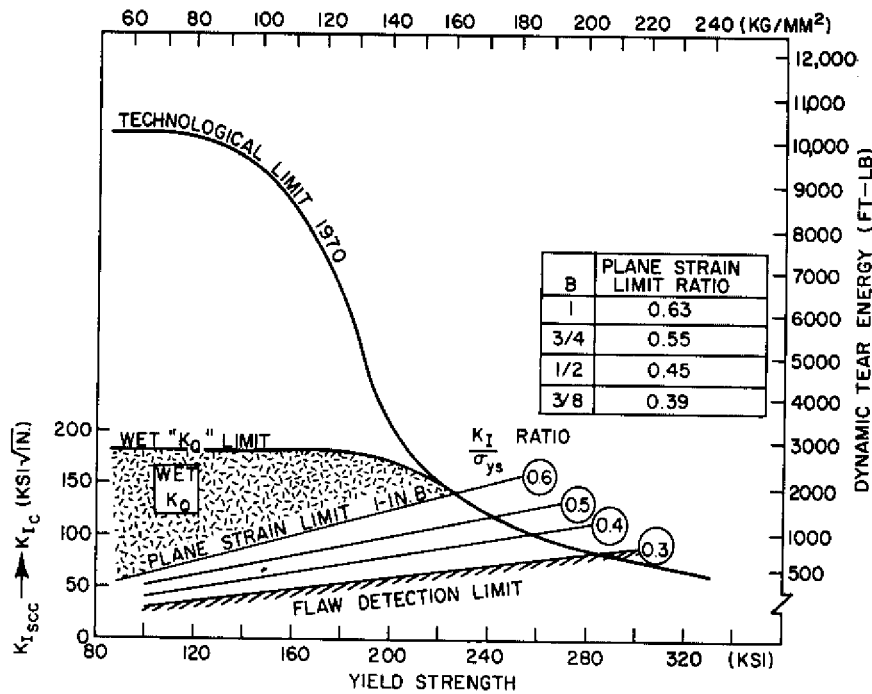


Fig. 10 — Dual-SCC RAD for steels

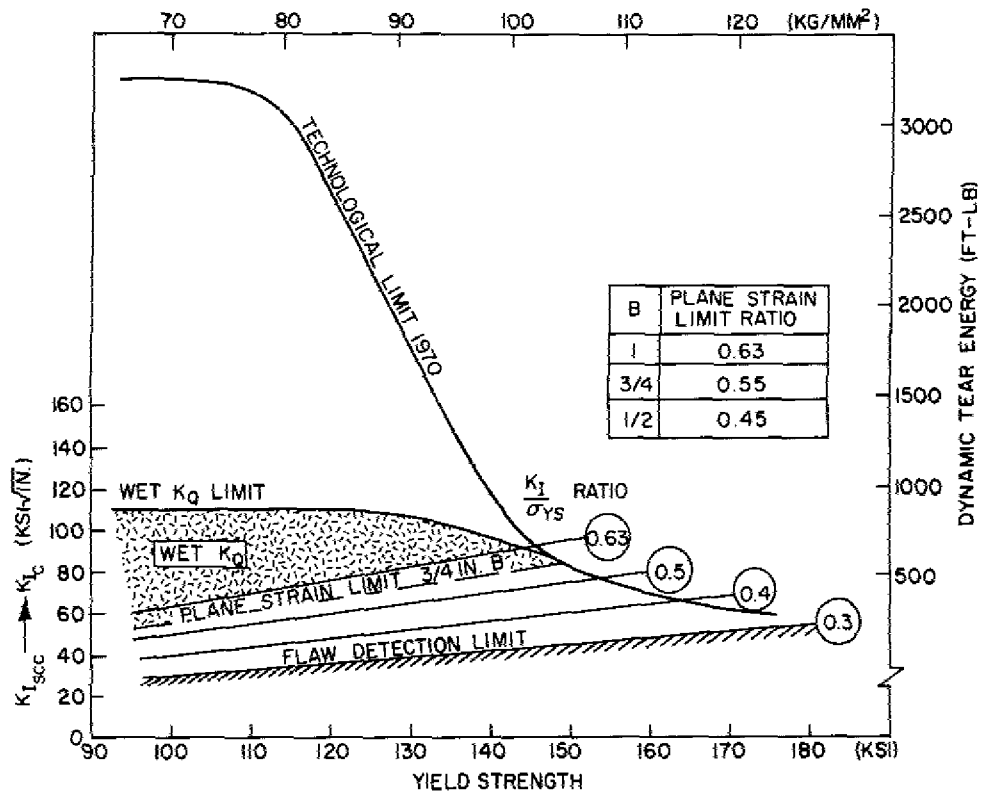


Fig. 11 — Dual-SCC RAD for titanium alloys

such values might result in an unacceptably conservative estimate of the capabilities of a material highly resistant to SCC, whereas overly optimistic estimates might result for sensitive materials.

The degree of degradation of a metal's resistance to the presence of flaws due to SCC sensitivity is indicated by comparing the location of the fast-fracture and SCC data points on this diagram. For this purpose, the K_{Isc}/σ_{ys} ratio is compared to the K_{Ic}/σ_{ys} ratio. If a metal of characteristically high fracture toughness has a low K_{Isc}/σ_{ys} ratio, extreme sensitivity to the environment is inferred. In this case, considerable SCC crack extension would occur before fast fracture because of the high fracture toughness of the material. Materials with a low level of inherent fracture toughness would withstand only a small amount of crack extension by SCC before the onset of fast fracture. SCC of very low-toughness materials (below ratio 0.5) is not really important for general design consideration, since the critical flaw size for fast fracture in these metals is minute.

ANALYSIS OF STEELS

Mechanical properties such as σ_{ys} , DT, K_{Ic} , and K_{Isc} can vary from point to point in a given plate and from one plate to another plate of the same nominal composition. Due to expected statistical variance of properties, a given alloy system is characterized by a representative range of these properties rather than by a single value. For this reason, materials on the RAD are represented by a zone reflecting the range of properties rather than by a point.

To simplify the interpretation of the effects of SCC, the Dual-SCC RAD can be divided into three ranges of σ_{ys} , as shown in Fig. 12 for the case of steel. Group I materials below 120 ksi σ_{ys} consist of HY-80, mild steels, etc., and generally feature fairly high levels of fast-fracture resistance. SCC is not a critical condition for most applications of these materials because of their high tolerance for large cracks at high stress levels. The presence of SCC poses a problem of inspection and repair of the structure rather than catastrophic failure, except for the rare case when metals with very high SCC crack propagation rates are involved.

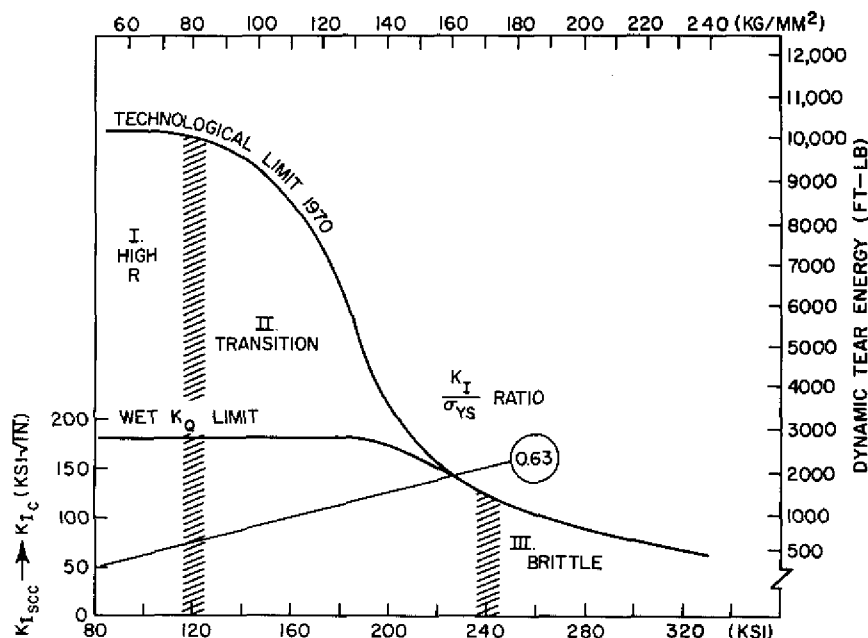


Fig. 12 — Steel Dual-SCC RAD zoned to show three regions: (I) SCC effects are minimal for most steels because of the inherent high tolerance of these materials to very large flaws, (II) transition of dry fracture resistance from high to low results in transition of potential SCC effects from minimal to severe, and (III) region where the presence of SCC is highly critical because of the criticality of small flaws.

Region II is the strength transition region which is outlined by the rapid decrease of the Technological Limit between yield strengths of 120 to 240 ksi. Materials range from high to low in fracture resistance and from completely immune to highly sensitive to environmental cracking in the transition region. Much of the steel data in this report fall in Region II because of a recent high level of research activity to develop usable steels in this strength range.

Region III consists of those materials above 240 ksi which are generally brittle. Any susceptibility of these materials to SCC precludes their use for structures designed with a close margin of allowable stress and flaw size. For Region III materials, critical flaw sizes are extremely small and even a small increment of crack growth can cause catastrophic fracture at low stress levels.

The range of properties representing the 5Ni-Cr-Mo-V system is shown on the Dual-SCC RAD, Fig. 13. It must be noted that the dry fracture toughness zone and the SCC zone on the Dual-SCC RADs of this report do not necessarily represent samples of the same plates in all cases; i.e., some materials in the fast-fracture zone may not be represented in the SCC zone. The dry fracture toughness of plate and weld metal products in the 5Ni-Cr-Mo-V system measured by the DT test is shown by the crosshatched zone. The SCC zone (dotted) represents all the K_{Isc} values available for the 5Ni alloy system. The location of the SCC zone in the Wet K_Q region shows that crack propagation by the mechanism of SCC is not expected for 5Ni steels, and definite evidence of SCC propagation in this material has not been reported. Thus, design based on the fracture resistance of this material is appropriate for aqueous environments. A marginal part of the SCC zone extends below the Wet K_Q region corresponding to extremely poor metallurgical quality material, but most of the data lie above the 1-in. plane-strain limit. The DT zone is sufficiently high in the RAD that the plate and weld metal samples would not fracture in the brittle mode in section sizes up to 3-in. thick for the materials in the lowest part of the zone. Materials at the middle and highest regions would not suffer brittle fracture in any thickness.

A similar situation exists for the 10Ni-8Co-2Cr-1Mo steel plate and weld metal samples shown in Fig. 14. The DT fracture resistance is entirely above the 1-in. plane-strain limit, and the SCC zone resides primarily in the Wet K_Q region. High SCC and ductile fracture resistance are expected for this steel when produced by vacuum melting techniques.

The Dual-SCC RAD for 9Ni-4Co-XC steels and weld metals normally produced by air melt followed by vacuum arc remelt (Fig. 15) shows that the resistance to fast fracture

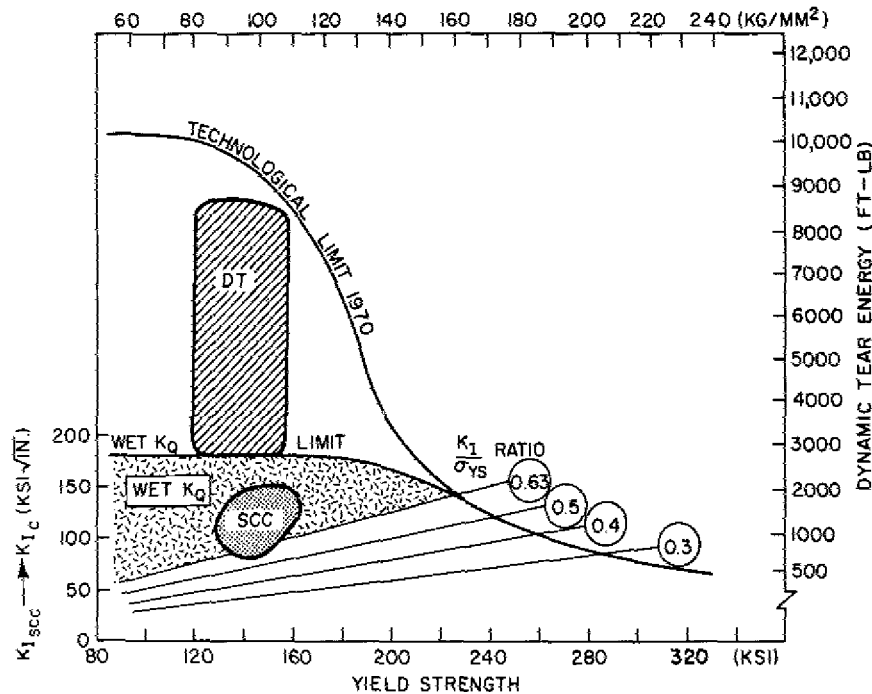


Fig. 13 — Dual-SCC RAD showing fast-fracture and SCC aspects of 5Ni-Cr-Mo-V steels and weld metals 1 in. thick

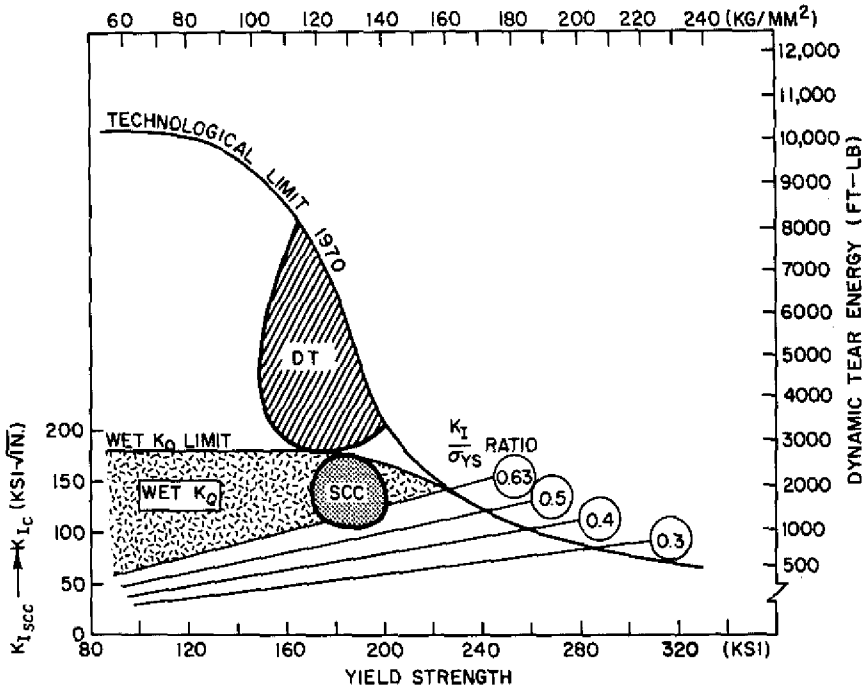


Fig. 14 — Dual-SCC RAD showing fast-fracture and SCC aspects of 10Ni-8Co-2Cr-1Mo steels and weld metals

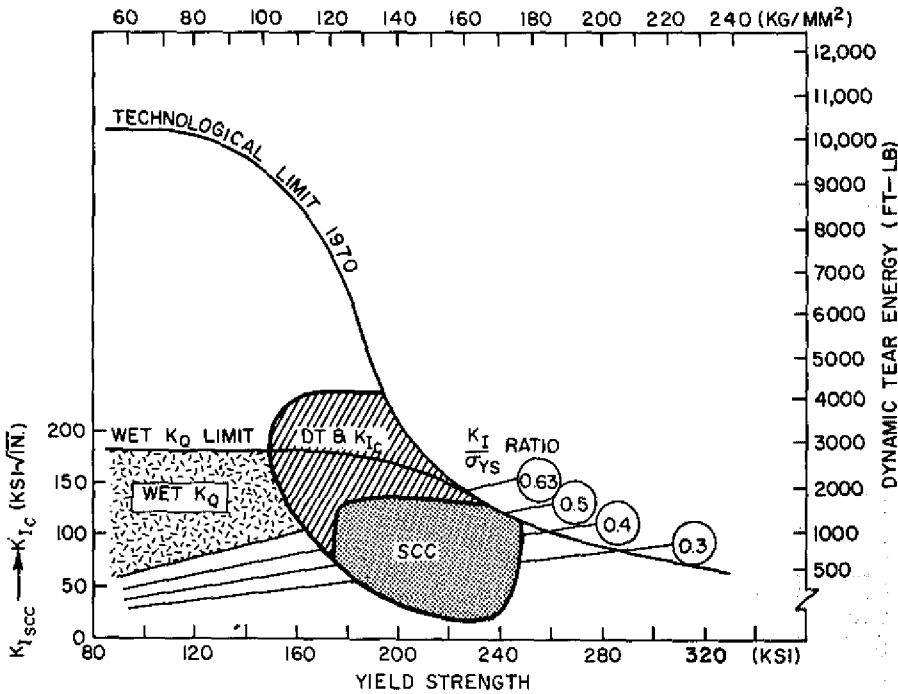


Fig. 15 — Dual-SCC RAD showing fast-fracture and SCC aspects of 9Ni-4Co-XC steels and weld metals 3/8 to 1 in. thick

for these steels can range from intermediate to very low. The SCC zone lies mostly below the Wet K_Q region so that the critical flaw size for either SCC or fast fracture is quite small.

A propensity for SCC is exhibited by the 12Ni-5Cr-3Mo family of steels (Fig. 16). The DT zone lies above the 1-in. plane-strain limit, while most of the SCC zone lies below the Wet K_Q region. This is an example of what the effects of the salt-water environment on an alloy system can be in terms of reducing the critical stress vs flaw condition from the intermediate levels evidenced in the upper region of the DT zone to very low values indicated by the SCC zone.

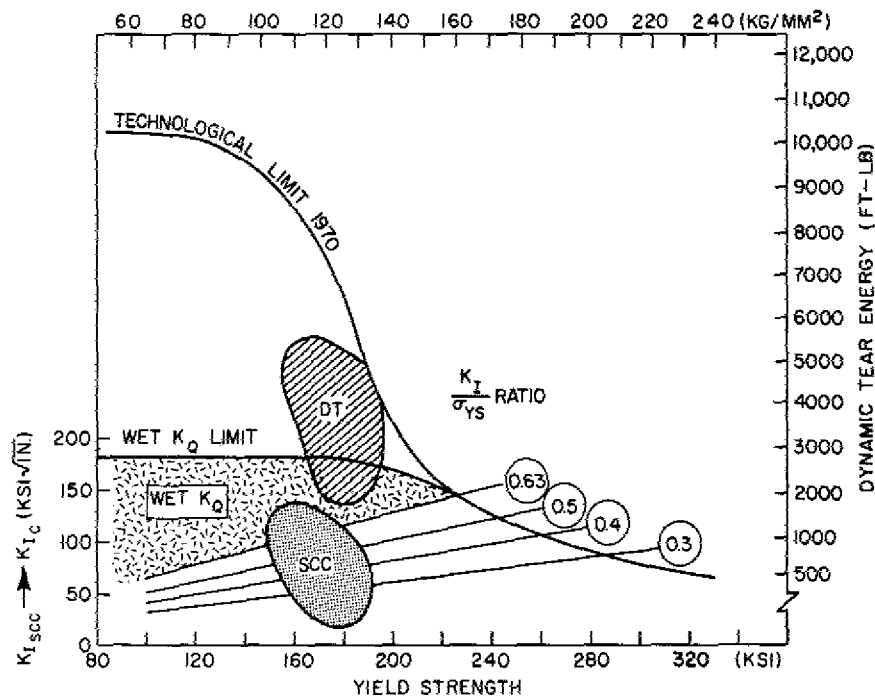


Fig. 16 — Dual-SCC RAD showing fast-fracture and SCC aspects of 12Ni-5Cr-3Mo steels and weld metals

A compendium of other steels is shown in Fig. 17. These steels are all high-strength alloys which, for the most part, evidence low levels of resistance to fast fracture and also have low values of K_{Isc} . Above approximately 240 ksi σ_{ys} , use of these materials on the basis of K_{Ic} and K_{Isc} values must be on a case basis for the reasons stated previously concerning inspectability problems and fracture due to minute flaws and low elastic stress levels.

ANALYSIS OF TITANIUM ALLOYS

Analyses of the fracture characteristics of titanium alloys are made from the Dual-SCC RAD in exactly the same fashion as for steels. Two materials that have very similar fast-fracture properties and very different SCC characteristics are shown in Fig. 18. Titanium alloys Ti-7Al-2Cb-1Ta (721) and Ti-6Al-2Cb-1Ta-0.8Mo (621-0.8) were developed

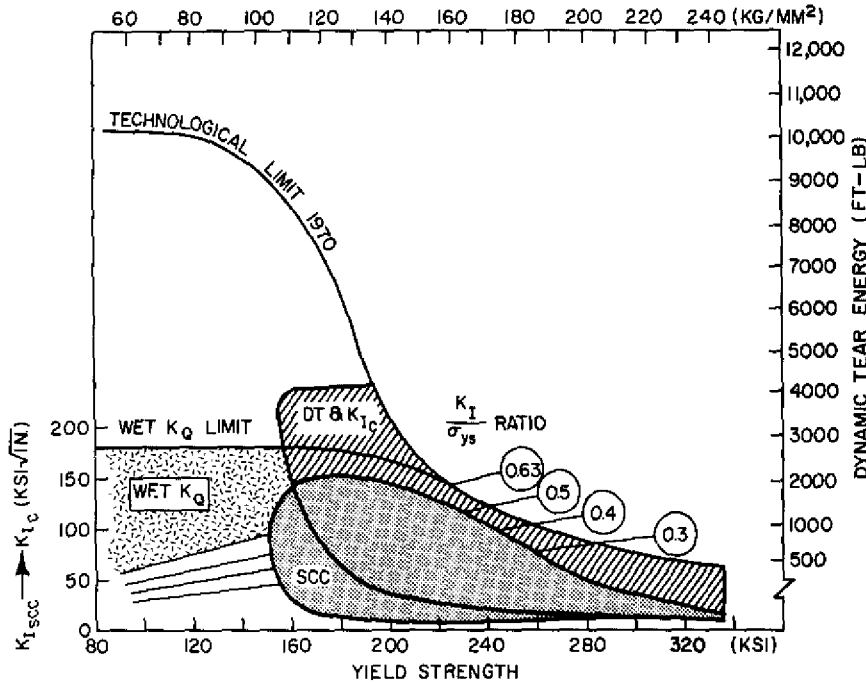


Fig. 17 - Dual-SCC RAD showing fast-fracture and SCC aspects of a group of ultrahigh strength 18Ni maraging steels - 4330, 4340, D6AC, and H11 - 3/8 in. thick

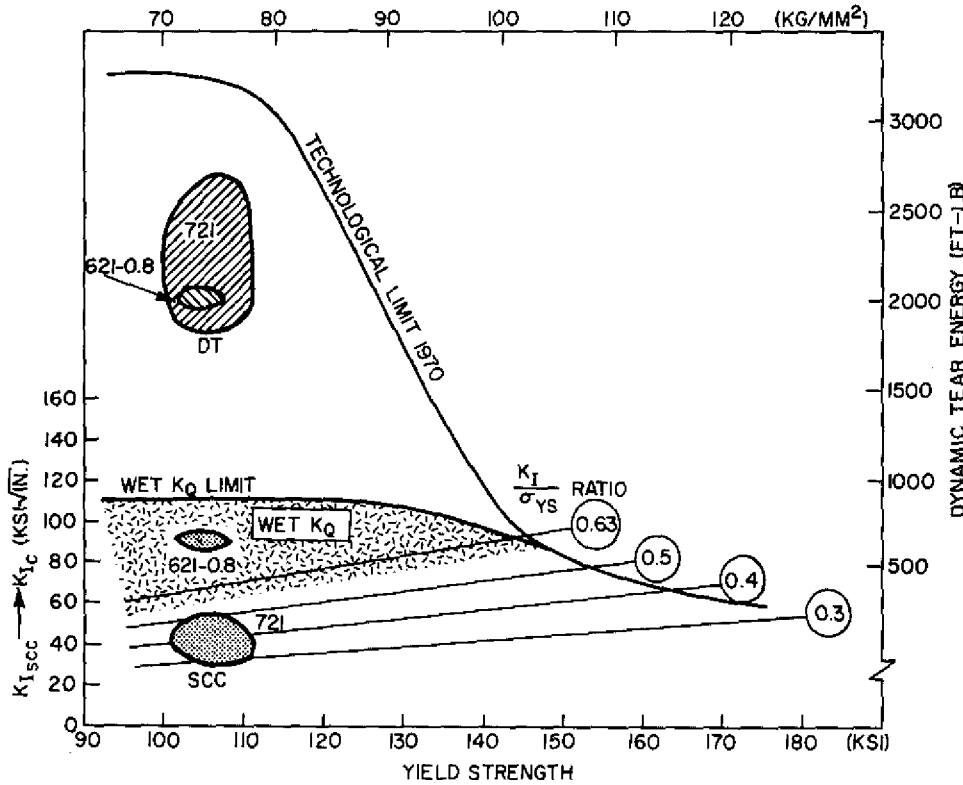


Fig. 18 - Dual-SCC RAD showing effects of salt-water environment on Ti-7Al-2Cb-1Ta and Ti-6Al-2Cb-1Ta-0.8Mo alloys

for structural applications in the Navy. A high degree of resistance to fast fracture for both alloys is shown to exist in the location of the DT zone very high in the ductile fracture region of the RAD. The susceptibility of the 721 alloy to salt-water SCC, indicated by the SCC zone, is well known. SCC cracks propagate at a very high rate in 721 so that this material cannot be used in a salt-water environment. A slight modification to the 721 chemistry resulted in the 621-0.8 composition which is insensitive to the salt-water environment.

Another well-known alloy that is sensitive to the salt-water environment is the Ti-5Al-2.5Sn system. The range of fast-fracture resistance illustrated by the zone in Fig. 19 points up the trend of decreasing fracture resistance with increasing yield strength. The SCC zone is lower than both the fast-fracture zone and the Wet K_Q region for all heat treatments reported, indicating a high degree of inherent SCC sensitivity for this alloy.

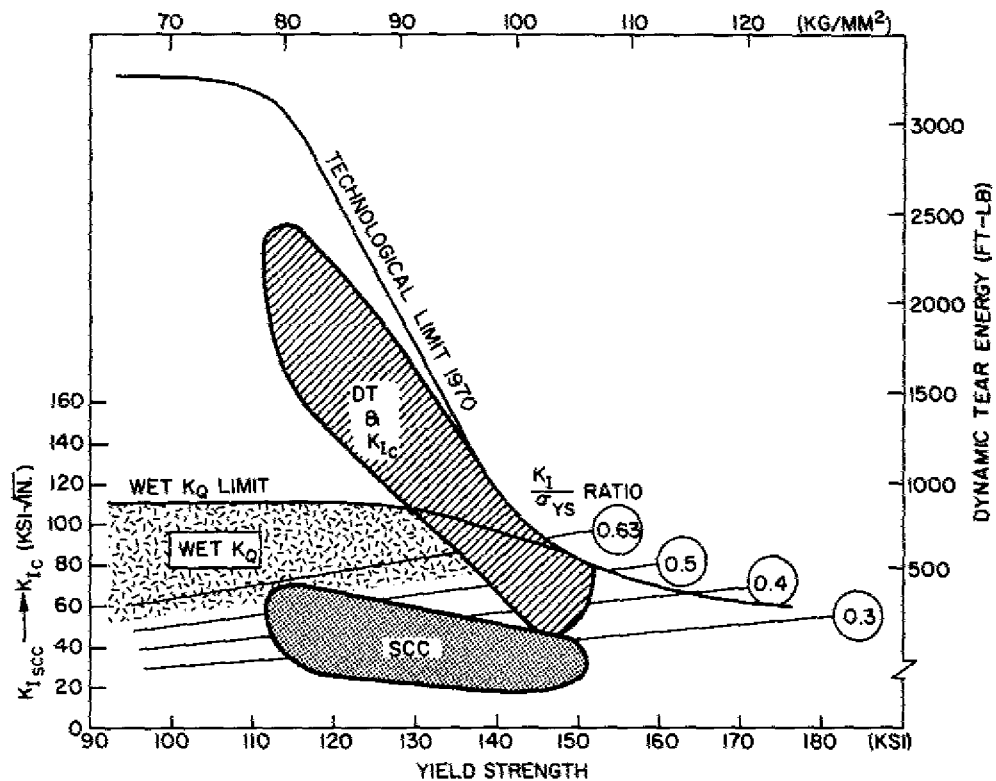


Fig. 19 — Dual-SCC RAD showing effects of salt-water environment on Ti-5Al-2.5Sn

A titanium alloy that is widely used, particularly by the aerospace industry, is Ti-6Al-4V (6-4). A great deal of work has been done with 6-4 so that the RAD zones, shown in Fig. 20, cover a wide range of properties. This alloy can be sensitive to SCC in salt water, as well as in other fluids, or it can be resistant, depending on several factors such as forging and rolling practices, heat treatment, impurity and oxygen contents, chemistry variations, etc. No general trend for 6-4 can be obtained by examining the Dual-SCC RAD because of the wide range of metal quality that is involved. Detailed analyses of the 6-4 material of concern must be made on a case basis, particularly by separation into quality zones as to fast-fracture vs SCC aspects.

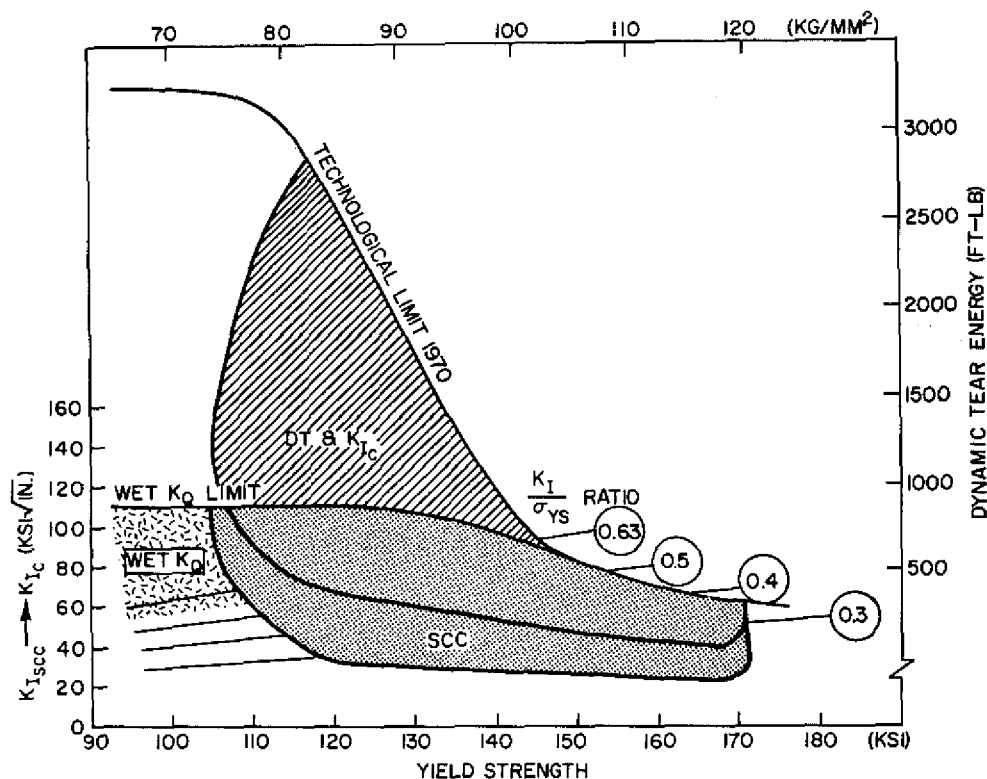


Fig. 20 — Dual-SCC RAD showing effects of salt-water environment on Ti-6Al-4V

Another titanium alloy system which has been investigated extensively because of its high resistance to fast fracture is the Ti-6Al-2Mo to Ti-7Al-2.5Mo composition range. The Dual-SCC RAD, Fig. 21, shows that a wide range of fast-fracture resistance can be obtained for this system by variation of the yield strength. No sensitivity of these alloys to SCC has been reported; however, the high strength-low toughness end of the fast-fracture zone has very low levels of fast-fracture resistance so that low K_{Isc} values are obtained. The lower values of K_{Isc} for this system were measured with specimens of 1/2-in. thickness, hence the Wet K_Q region is bounded by the 0.45 K_{Isc}/σ_{ys} ratio line. Due to previously described effects of loading specimens over a period of time, the K_{Isc} zone extends below even this Wet K_Q region without the presence of SCC.

A group of titanium alloys for which only K_{Isc} data are available is shown in Fig. 22. These alloys are typical of the three σ_{ys} regions of the RAD previously described for steels. The Ti-4Al-4Mo-2Sn-5Si system has a yield strength range of 140 to 180 ksi, which limits the fast-fracture resistance to very low levels and thereby restricts K_{Isc} values to the same low levels. The Ti-5Al-5Sn-5Zr system ranges from 110 to 135 ksi yield strength, which corresponds generally to the range where high fracture resistance is expected. The low position of the SCC zone for this chemical composition is evidence of high SCC sensitivity. The Ti-4Al-3Mo-1V alloys system ranges from 125 to 170 ksi σ_{ys} , covering the strength transition defined by the Technological Limit line. As expected, the SCC zone ranges from the Wet K_Q limit at the low σ_{ys} levels to very low K_{Isc} values at high σ_{ys} levels.

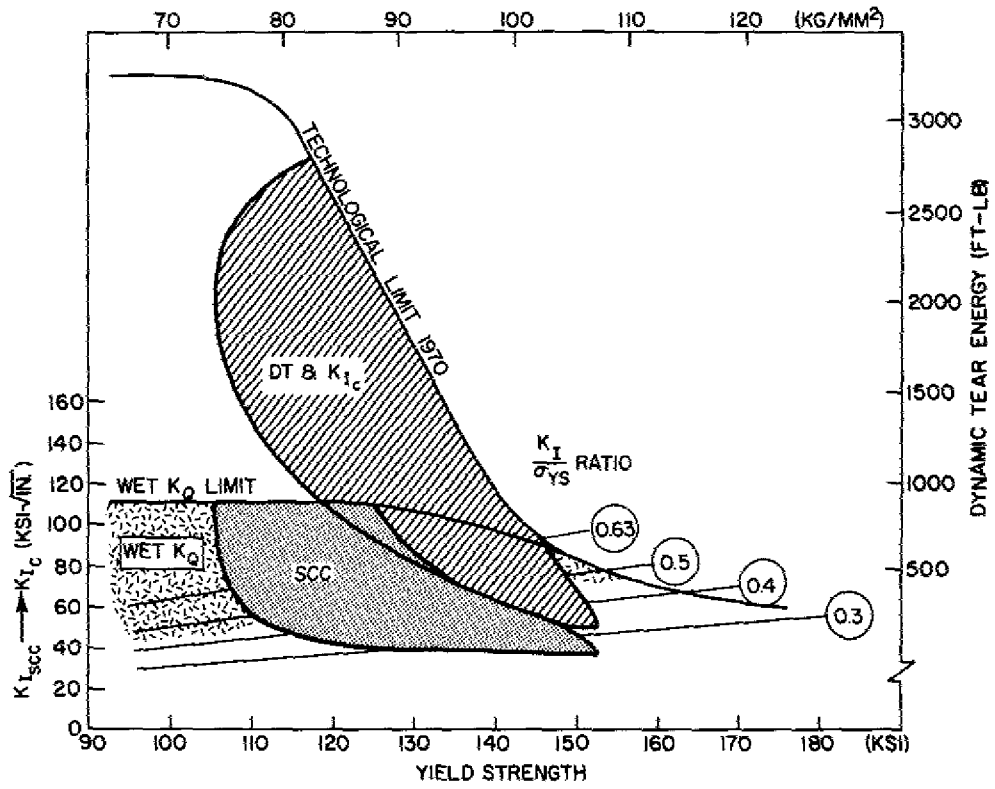


Fig. 21 — Dual-SCC RAD showing effects of salt-water environment on Ti-6Al-2Mo and Ti-7Al-2.5Mo

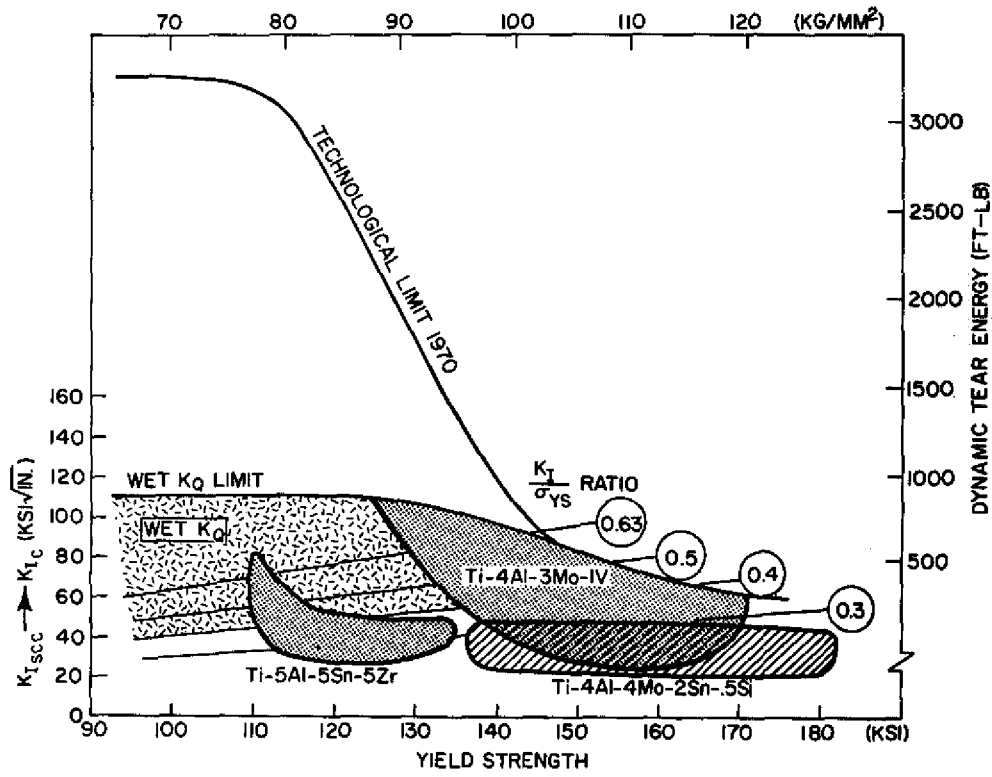


Fig. 22 — Dual-SCC RAD showing effects of salt-water environment on several titanium alloys where adequate fast-fracture data were not available

SUMMARY

An investigation of the spectrum of high-strength steels and titanium alloys available for structural applications reveals a wide range of SCC behavior in salt water. Tests based on linear-elastic fracture mechanics methods provide the best definition of SCC resistance in terms of a crack-tip stress-intensity parameter K_I . The minimum (threshold) value of K_I for SCC to occur is termed $K_{I_{SCC}}$. Essentially any plane-strain fracture mechanics test can be used to determine $K_{I_{SCC}}$; regardless of which fracture mechanics test is used, the thickness B requirement is critical for valid $K_{I_{SCC}}$ measurements. Flaw size vs stress conditions for subcritical crack growth due to SCC can be calculated from the $K_{I_{SCC}}$ value.

Ratio Analysis Diagram procedures have been established for characterization of materials' resistance to fast fracture and to interpret these for failure-safe design. To cover the case for SCC in high-strength titanium alloys and high-strength steels, the Dual-SCC RAD provides engineering definitions of flaw size vs stress conditions for failure by subcritical crack propagation. The Wet K_Q limit line defines the highest $K_{I_{SCC}}$ values obtained with 1-in.-thick precracked fracture mechanics specimens. The plane-strain limit lines for SCC indicate the upper limit of valid $K_{I_{SCC}}$ measurement as well as accurate $K_{I_{SCC}}/\sigma_{ys}$ ratio interpretation to flaw size vs stress conditions for SCC. A Wet K_Q region of full and mixed-mode plane stress is defined by the Wet K_Q and plane strain limit lines for which SCC may occur in the plane-strain (central) portion of the specimen. Accurate K_I/σ_{ys} ratio interpretations to flaw size vs stress conditions for SCC cannot be made for this region.

The severity of environmental effects can be determined only by comparison of fast-fracture resistance and SCC resistance in terms of the flaw size vs stress level conditions, as defined by the K_I/σ_{ys} ratios, that are critical for each case. The Dual-SCC RAD facilitates such comparisons by providing a format utilizing this common parameter.

Dual-SCC RAD analyses for several high-strength steels and titanium alloys were presented; these represented recent and current research and commercial grades of high-strength materials for which SCC data could be found. By examining the data on the Dual-SCC RAD, it was concluded that effects of sensitivity to salt-water SCC were to reduce the flaw size that could be tolerated to a very small value. In many cases, the low fast-fracture toughness level inherent in the material resulted in the low values of $K_{I_{SCC}}$ that could be erroneously attributed to SCC effects. In most cases, whether SCC sensitivity is present depends highly upon such factors as heat treatment, processing practices, etc. For these reasons, case-by-case testing for SCC sensitivity is necessary for new materials used in specific heat-treated conditions to assure that crack propagation due to the environment will not occur.

REFERENCES

1. Novak, S.R., and Rolfe, S.T., "Comparison of Fracture-Mechanics and Nominal-Stress Analyses in Stress-Corrosion Testing," U.S. Steel Applied Research Laboratory Report 89.018-026(3) B-63105, Dec. 20, 1968
2. Smith, H.R., Piper, D.E., and Downey, F.K., "A Study of Stress-Corrosion Cracking by Wedge-Force Loading," Eng. Fracture Mec. 1:123 (1968)

3. Brown, B.F., "A New Stress-Corrosion Cracking Test for High-Strength Alloys," *Mater. Res. Stand.* 6(No. 3):129-133 (1966)
4. Novak, S.R., and Rolfe, S.T., "Modified WOL Specimen for K_{Isc} Environmental Testing," U.S. Steel Applied Research Laboratory Report 89.018-026(1), May 31, 1968
5. Tentative Method of Test for Plane-Strain Fracture Toughness of Metallic Materials, ASTM Designation E399-70T
6. Pellini, W.S., and Judy, R.W., Jr., "Significance of Fracture Extension Resistance (R Curve) Factors in Fracture-Safe Design for Nonfrangible Metals," *Welding Res. Counc. Bull.* 157, Dec. 1970; also NRL Report 7187, Oct. 19, 1970
7. Judy, R.W., Jr., and Goode, R.J., "Fracture Extension Resistance (R Curve) Concepts for Fracture-Safe Design with Nonfrangible Titanium Alloys," NRL Report 7313, Aug. 16, 1971
8. Goode, R.J., and Judy, R.W., Jr., "Fracture Extension Resistance (R Curve) Features of Nonfrangible Aluminum Alloys," NRL Report 7262, June 11, 1971
9. Pellini, W.S., "Integration of Analytical Procedures for Fracture-Safe Design of Metal Structures," NRL Report 7251, Mar. 26, 1971
10. Pellini, W.S., "Advances in Fracture Toughness Characterization Procedures and in Quantitative Interpretations to Fracture-Safe Design for Structural Steels," *Welding Res. Counc. Bull.* 130, 1968; also NRL Report 6713, Apr. 1968
11. Goode, R.J., Judy, R.W., Jr., and Huber, R.W., "Procedures for Fracture Toughness Characterization and Interpretations to Failure-Safe Design for Structural Titanium Alloys," *Welding Res. Counc. Bull.* 134, Oct. 1968; also NRL Report 6779, Dec. 1968
12. Judy, R.W., Jr., Goode, R.J., and Freed, C.N., "Fracture Toughness Characterization Procedures and Interpretations to Fracture-Safe Design for Structural Aluminum Alloys," *Welding Res. Counc. Bull.* 140, May 1969; also NRL Report 6871, Mar. 1969
13. Judy, R.W., Jr., and Goode, R.J., "Procedures for Stress-Corrosion Cracking Characterization and Interpretation to Failure-Safe Design for High-Strength Steels," NRL Report 6988, Nov. 29, 1969; also published as "Failure-Safe Design with High-Strength Steels for Salt Water Applications," *Proc. 1970 NACE Conf., Materials Protection and Performance*, Aug. 1970, Vol. 9 (No. 8), pp. 23-29
14. Judy, R.W., Jr., and Goode, R.J., "Stress-Corrosion-Cracking Characterization Procedures and Interpretations to Failure-Safe Use of Titanium Alloys," NRL Report 6879, Apr. 8, 1969; also *ASME Trans., J. Basic Eng.* 91 (Series D, No. 4):614 (Dec. 1969)
15. Novak, S.R., and Rolfe, S.T., " K_{Ic} Stress-Corrosion Tests of 12Ni-5Cr-3Mo and 18Ni-8Co-3Mo Maraging Steels and Weldments," U.S. Steel Applied Research Laboratory Report 39.018-002(34) (S-23309-2), Jan. 1, 1966
16. Benjamin, W.D., and Steigerwald, E.A., "Stress Corrosion Cracking Mechanisms in Martensitic High Strength Steels," Air Force Materials Laboratory Technical Report TR-67-98, Apr. 1967
17. Peterson, M.H., Brown, B.F., Newbegin, R.L., and Groover, R.E., "Stress Corrosion Cracking of High Strength Steels and Titanium Alloys in Chloride Solutions at Ambient Temperature," *Corrosion* 23 (No. 5):142-148 (May 1967)

18. Novak, S.R., and Rolfe, S.T., "K_{Isc} Tests of HY-180/210 Steels and Weld Metals," U.S. Steel Applied Research Laboratory Report 39.018-007 (12) (B-63105, B63304), Aug. 1, 1967
19. Novak, S.R., "Effect of Plastic Strain on the K_{Isc} of HY-80, HY-130(T) and 12Ni-5Cr-3Mo Steels," U.S. Steel Applied Research Laboratory Report 39.018-007 (20) (B-63201), Jan. 1, 1968
20. Smith, J.H., and Rolfe, S.T., "Effects of Welding Position and Process on the K_{Isc} of HY-130(T) Weld Metals," U.S. Steel Applied Research Laboratory Report 39.018-016 (7) (B-33204), Jan. 1, 1968
21. Connor, L.P., Porter, L.F., and Rolfe, S.T., "Third Progress Report: Development of an HY-180/210 Weldment," U.S. Applied Research Laboratory Report 39.018-007 (21) (B-60000-2), Jan. 1, 1968
22. Smith, J.H., and Rolfe, S.T., "K_{Isc} Behavior of Weld Metals Used in Fabrication of an HY-130 (T) Steel Structure," U.S. Steel Applied Research Laboratory Report 39.018-015 (4) (B-10000-3), Jan. 1, 1968
23. Smith, J.H., and Rolfe, S.T., "Effect of Composition on the K_{Isc} of Experimental HY-150 Steels," U.S. Steel Applied Research Laboratory Report 39.018-016 (10) (B-23104), Dec. 20, 1968
24. Dabkowski, D.S., Konkoi, P.J., Novak, S.R., and Porter, L.F., "Evaluation of the HY-9-4-20 Steel Weldment System," U.S. Steel Applied Research Laboratory Report 39.018-007 (30) (B-61209-1), Jan. 2, 1969
25. Webster, D., "The Use of Deformation Voids to Refine the Austenite Grain Size and Improve the Mechanical Properties of AFC 77," The Boeing Company Document D6-23879, Feb. 1969
26. Carter, C.S., "Stress Corrosion Crack Branching in High Strength Steels," presented at ASM/WESTEC Conf., Los Angeles, Calif.; Boeing Document D6-23871, Mar. 1969
27. Carter, C.S., "The Effect of Silicon on the Stress Corrosion Cracking Resistance of Low Alloy High Strength Steels," Boeing Document D6-23872, Mar. 1969
28. Sandoz, G., and Newbegin, R.L., "Stress-Corrosion Cracking Resistance of an 18Ni-200 Grade Maraging Steel Base Plate and Weld," NRL Memorandum Report 1772, Mar. 1967
29. Novak, S.R., "Comprehensive Investigation of the K_{Isc} Behavior of Candidate HY-180/210 Steel Weldments," U.S. Steel Applied Research Laboratory Report 89.021-024 (1) B63105, Dec. 31, 1970
30. Smith, J.H., and Davis, J.A., "Stress Corrosion and Hydrogen Embrittlement Cracking Behavior of HY-80 and HY-130 Weld Metals," U.S. Steel Applied Research Laboratory Report 89.021-024 (4) B-63304, Jan. 22, 1971
31. Bieffer, G.J., and Garrison, J.G., "Stress Corrosion Cracking Tests on Some High Strength Steels Using the U.S.N. Cantilever Method," Internal Report PM-R-67 Physical Metallurgy Division, Dept. of Energy, Mines and Resources, Mines Branch, Ottawa, Canada, Mar. 14, 1967
32. Sandoz, G., and Brown, B.F., unpublished data

33. Judy, R.W., Jr., and Goode, R.J., "Stress-Corrosion Cracking Characteristics of Alloys of Titanium in Salt Water," NRL Report 6564, July 21, 1967
34. Fager, D.N., and Spurr, W.F., "Some Characteristics of Aqueous Stress-Corrosion in Titanium Alloys," ASM Trans. Quart. 61:283 (June 1968)
35. Curtis, R.E., Boyer, R.R., and Williams, J.C., "Relationship Between Composition, Microstructure, and Stress Corrosion Cracking (in Salt Solution) in Titanium Alloys," ASM Trans. Quart. 62:457 (June 1969)
36. "ARPA Coupling Program on Stress Corrosion Cracking (Fourth Quarterly Report)," NRL Memorandum Report 1834, Nov. 1967; and Seventh Quarterly Report, NRL Memorandum Report 1941, Oct. 1968